Molecular Cell
Article

Disease-Associated Prion Protein Oligomers Inhibit the 26S Proteasome

Mark Kristiansen,[1,2,6] Pelagia Deriziotis,[2,6] Derek E. Dimcheff,[3,7] Graham S. Jackson,[1,7] Huib Ovaa,[4] Heike Naumann,[1] Anthony R. Clarke,[1] Fijs W.B. van Leeuwen,[4] Victoria Menéndez-Benito,[5] Nico P. Dantuma,[5] John L. Portis,[3] John Collinge,[1,2] and Sarah J. Tabrizi[2,*]
[1] MRC Prion Unit
[2] Department of Neurodegenerative Disease
Institute of Neurology, University College London, Queen Square, London WC1N 3BG, UK
[3] Laboratory of Persistent Viral Diseases, NIAID, NIH Rocky Mountain Laboratories, 903 South 4th Street, Hamilton, MT 59840, USA
[4] Division of Cellular Biochemistry, Netherlands Cancer Institute, Plesmanlaan 121, 1066 CX Amsterdam, Netherlands
[5] Department of Cell and Molecular Biology, Karolinska Institutet, P.O. Box 285, Von Eulers väg 3, S-171 77 Stockholm, Sweden
[6] These authors contributed equally to this work.
[7] These authors contributed equally to this work.
*Correspondence: sarah.tabrizi@prion.ucl.ac.uk
DOI 10.1016/j.molcel.2007.04.001

SUMMARY

The mechanism of cell death in prion disease is unknown but is associated with the production of a misfolded conformer of the prion protein. We report that disease-associated prion protein specifically inhibits the proteolytic β subunits of the 26S proteasome. Using reporter substrates, fluorogenic peptides, and an activity probe for the β subunits, this inhibitory effect was demonstrated in pure 26S proteasome and three different cell lines. By challenge with recombinant prion and other amyloidogenic proteins, we demonstrate that only the prion protein in a nonnative β sheet conformation inhibits the 26S proteasome at stoichiometric concentrations. Preincubation with an antibody specific for aggregation intermediates abrogates this inhibition, consistent with an oligomeric species mediating this effect. We also present evidence for a direct relationship between prion neuropathology and impairment of the ubiquitin-proteasome system (UPS) in prion-infected UPS-reporter mice. Together, these data suggest a mechanism for intracellular neurotoxicity mediated by oligomers of misfolded prion protein.

INTRODUCTION

Prion diseases are fatal neurodegenerative disorders whose pathogenesis is associated with a conformational rearrangement of the normal cellular prion protein (PrP^{C}) to abnormal conformers (PrP^{Sc}) (Prusiner, 1982). PrP^{C} is soluble, monomeric, and rich in α-helical structure, whereas the disease-associated PrP^{Sc} is characterized by increased β sheet structure, detergent insolubility, and partial resistance to proteolysis. Neuropathologically, prion diseases are characterized by severe neuronal loss, marked gliosis, and spongiform change and accumulation of PrP^{Sc} in the brain. However, the cause of prion-mediated neurodegeneration is not known, and a major gap exists in the understanding of how the conversion of PrP^{C} to PrP^{Sc} ultimately kills neurons. It is known that PrP^{C} is essential for the development of prion disease (Bueler et al., 1993). However, loss of function of PrP^{C} is unlikely to be the cause of prion-mediated pathology because neither embryonic (Bueler et al., 1993) nor adult knockout (Mallucci et al., 2002) of PrP^{C} results in neurodegeneration. Hence, an unknown toxic gain of function of PrP^{Sc} or its precursor is more likely to underlie this characteristic pathology.

There is increasing evidence that intracellular PrP^{Sc} accumulation in neurons may be necessary to cause toxicity. First, neurons that do not express PrP^{C}, and therefore cannot produce PrP^{Sc}, remain healthy and free of pathology (Brandner et al., 1996; Mallucci et al., 2003). Second, prion-infected transgenic mice expressing PrP lacking its glycosylphosphatidylinositol (GPI) anchor produced infectious prions and accumulated PrP amyloid plaques in their brains but did not succumb to clinical disease (Chesebro et al., 2005).

Various mechanisms have been proposed to explain neuronal death in prion disease (Caughey and Baron, 2006; Harris and True, 2006). In vitro studies have suggested that both full-length PrP^{Sc} (Hetz et al., 2003) and shorter peptide fragments (Forloni et al., 1993) are toxic when applied to primary neurons. Other mechanisms suggested relate to altered PrP^{C} trafficking. It has been described that PrP^{C} may assume a transmembrane topology (^{Ctm}PrP), which has been suggested to correlate with neurotoxicity (Hegde et al., 1998). It has been proposed that toxicity involves altered trafficking of PrP^{C}, where inhibition of the UPS results in cytosolic PrP^{C} accumulation and cell death (Ma and Lindquist, 2002). Our previous

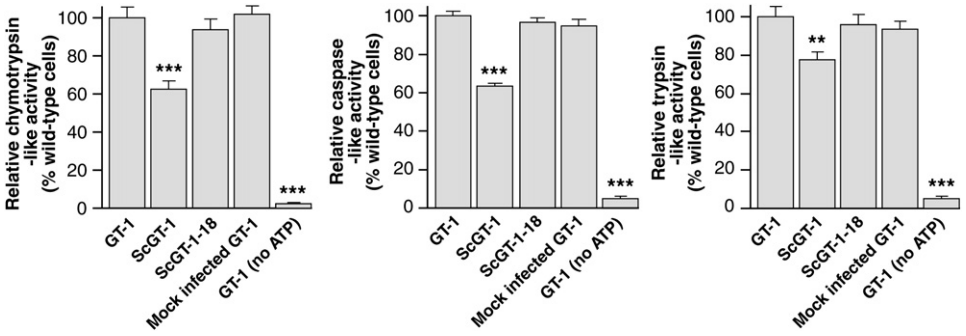

Figure 1. Prion Infection Impairs the Proteolytic Activity of the 26S Proteasome
Prion infection significantly reduces proteolytic activities in ScGT-1 cells. Suffix −18 denotes cells cured of prion infection. n = 10 ± SEM.

work has suggested a clear role for UPS dysfunction in the pathogenesis of prion disease. We found that neuronal propagation of prions in the presence of mild proteasome impairment invoked a neurotoxic mechanism involving the intracellular formation of cytosolic PrP^{Sc} aggresomes that triggered caspase-dependent neuronal apoptosis with evidence for similar structures in vivo in brains of prion-infected mice (Kristiansen et al., 2005).

Degradation of intracellular proteins via the UPS is a complex and tightly regulated process that plays a critical role in a variety of cellular processes (Goldberg, 2003). The 26S proteasome is an ATP-dependent complex that consists of a 20S proteolytic core complexed at one or both ends with a 19S regulatory complex (Goldberg, 2003). The 20S proteasome is a hollow, barrel-shaped protein complex composed of 14 α and 14 β subunits arranged in four stacked rings with an overall architecture of α(1–7)β(1–7)β(1–7)α(1–7) (Hershko and Ciechanover, 1998). The two outer α rings form gated channels through which substrates enter and products exit the catalytic core. The proteolytic activity of the 20S proteasome resides in the two inner β rings. The proteasome has three distinct catalytic activities, each of which can be correlated to the action of an individual β subunit. These are termed β1 (caspase-like), β2 (trypsin-like), and β5 (chymotrypsin-like), and the secondary alcohol of the N-terminal threonine of the active β subunit acts as the nucleophilic species (Voges et al., 1999). By recognizing and selectively degrading misfolded and damaged proteins, the UPS protects cells against the potentially toxic effects of protein aggregation. Aberrations in this system have been implicated in the pathogenesis of Parkinson's disease, Alzheimer's disease, and Huntington's disease (HD) (Ciechanover and Brundin, 2003). The proteasome cannot efficiently degrade aggregated protein (Verhoef et al., 2002), and protein aggregates have been shown to actually impair the functional capacity of the UPS in cell models (Bence et al., 2001). Currently, the role of the UPS in these neurodegenerative diseases is debated. In a spinocerebellar ataxia 7 (SCA7) mouse model, polyglutamine pathogenesis occurred in the absence of significant proteasome impairment (Bowman et al., 2005); in an HD mouse model, there was no detectable impairment of proteasome function (Bett et al., 2006). An alternative route for cellular protein clearance is via autophagy, and data suggest that many aggregation-prone proteins can also be cleared via this mechanism (Rubinsztein, 2006).

The aims of this study were to examine further the nature of the PrP species responsible for neurotoxicity, to evaluate the role of the UPS in prion disease pathogenesis, and to investigate whether there was a direct mechanistic link between the two. We have shown in vitro that purified PrP^{Sc} preparations impair neuronal cellular function by inhibiting the catalytic core β subunits of the 26S proteasome; a recombinant aggregated β sheet-rich protein that shares many physico-chemical properties with PrP^{Sc}, designated β-PrP (Jackson et al., 1999b), has a similar effect at stoichiometric concentrations. Preincubation with an antibody specific for small aggregation intermediates abrogates this inhibition, consistent with the hypothesis that a small oligomeric PrP species mediates this effect. We also present in vivo evidence for a direct relationship between prion neuropathology and proteasome inhibition by using a reporter mouse model for the UPS. To the best of our knowledge, this is the first reported in vivo evidence for functional proteasome impairment in a neurodegenerative disease characterized by protein aggregation. These data together suggest a mechanism for intracellular prion-mediated neurotoxicity.

RESULTS

Prion Infection Impairs the Proteolytic Activity of the 26S Proteasome

Mouse hypothalamic neuronal GT-1 (Schatzl et al., 1997) and neuroblastoma N2aPK-1 cells (Klohn et al., 2003) were infected with either RML prion-infected or mock-infected CD-1 mouse brain homogenate (Figure S1A in the Supplemental Data available with this article online). Chymotrypsin-like, caspase-like, and trypsin-like proteolytic activities were measured in prion-infected, mock-infected, and wild-type GT-1 and N2aPK-1 cells. Significant loss of chymotrypsin-like (38%) and caspase-like activity (37%) was seen in ScGT-1 cells (Figure 1) and

also in ScN2aPK-1 cells (data not shown). Assays in the absence of ATP showed no activity, confirming measurement of proteolytic activity of the ATP-dependent 26S proteasome (Figure 1). Normal proteolytic activities were seen in mock-infected cells and cells cured of prion infection by using anti-PrP monoclonal antibody treatment (Figure 1). Measurement of proteasome activity in RML-prion-infected CD-1 mouse brain (Figure S1B) demonstrated significant loss of chymotrypsin-like and caspase-like activity (Figure S1C). Immunoblotting for proteasome subunits revealed no loss of subunits, indicating that loss of proteolytic activity results from an inhibitory effect (Figure S1D). However, assaying proteasomal function from prion-infected brain is complicated by the presence of the marked glial proliferation characteristic of prion neuropathology, which may result in overestimation of proteolytic function. Therefore, we studied proteasome reporter mice inoculated with prions (see below). In summary, prion infection results in loss of the chymotrypsin-like and caspase-like proteolytic activities in two different neuronal cell lines and prion-infected mouse brain.

Cytosolic Localization of PrP^{Sc} in Prion-Infected Cells

Because the proteasome is localized in the nucleus and cytosol of cells, we probed whether PrP^{Sc} accesses the cytosol in prion-infected cells. Due to the lack of PrP^{Sc}-specific antibodies, the subcellular distribution of PrP^{Sc} is difficult to assess. Studies support localization at the plasma membrane and in the endolysosomal compartment (Caughey and Baron, 2006). Using formic acid (FA) pretreatment to remove all PrP^{C} (Kristiansen et al., 2005), we show PrP^{Sc} on the cell surface and intracellularly in ScN2aPK-1 cells (Figure S2A). Dual-labeled immunostaining shows PrP^{Sc} partially colocalized with the endolysosomal marker LAMP-1, but it also exists outside this compartment (Figure 2A). We also show that a proportion of FA-resistant PrP^{Sc} colocalizes with the cytosolic marker Hsc70 (Figure 2B). An intensity scatter plot and subtraction image (Figure S2B) reveals true colocalization between Hsc70 and PrP^{Sc}. The presence of a proportion of cytosolic PrP^{Sc} is supported by our previous data describing neurotoxic cytosolic PrP^{Sc} aggresomes (Kristiansen et al., 2005). These data show a limited amount of PrP^{Sc} is present in the cytosol in prion-infected cells.

Prion Infection Results in Malfunction of the Intact Proteasome in Live Cells

To test whether the proteolytic dysfunction observed in prion-infected neuronal cells resulted in functional impairment of the UPS in live cells, we infected an N2aPK-1 cell line stably expressing the fluorescent proteasome reporter substrate Ub^{G76V}-GFP (Dantuma et al., 2000) with prions. Prion infection caused an increase in the steady-state levels of the reporter indicative of functional impairment of the UPS (Figure 2C). Curing cells of prion infection resulted in normal UPS function (Figure 2C). We followed the ability of cells to clear the reporter that had been accumulated by incubation with a reversible proteasome inhibitor. Prion-infected cells took significantly longer to clear the reporter than uninfected cells (Figure 2D). The rate of degradation at 1 hr was 42% less in prion-infected cells (Figure S3A). Using cycloheximide, an inhibitor of protein synthesis, still resulted in a delay in degradation of the reporter, indicating impaired proteolytic function (Figure S3B).

PrP^{Sc} and Aggregated Recombinant β-PrP Inhibit Proteolysis by the 26S Proteasome

To investigate a possible role for PrP species in UPS inhibition, we developed an in vitro assay system to measure the effects of different conformations and aggregation states of PrP on 26S proteasome activity, both in pure form and in neuronal cell lysates. Recombinant mouse PrP (aa 23–231) was used folded into either an α-helical structure representative of native PrP^{C} (α-PrP) or a predominantly β sheet species termed β-PrP (Jackson et al., 1999b). We have previously shown that β-PrP has similar physico-chemical properties to PrP^{Sc} (Jackson et al., 1999b). We made five different PrP species: aggregated α-PrP, aggregated β-PrP, which forms small, spherical particles 5–10 nm in diameter (Jackson et al., 1999b), acidified α-PrP-derived amyloid fibrils (Baskakov et al., 2002), and NaCl-treated α-PrP. We also studied semipurified PrP^{Sc} from RML-infected CD-1 mouse brain and ScGT-1 cells (Kristiansen et al., 2005).

In pure 26S proteasome assays, only aggregated β-PrP and PrP^{Sc} caused a significant reduction in chymotrypsin-like (Figure 3Aa; β-PrP, 56% loss; PrP^{Sc}, 42%) and caspase-like activity (Figure 3Ab; β-PrP, 56%; PrP^{Sc}, 47%). They had a lesser but still significant effect on trypsin-like activity (Figure 3Ac). None of the other PrP species above had any inhibitory effect on proteolytic activity (Figures 3Aa–3Ac). We assayed 26S proteasome activity in lysates from GT-1, N2aPK-1 cells, and in primary cerebellar granule neurons (CGNs). Only aggregated β-PrP and PrP^{Sc}, but not the other prion species, caused a significant reduction in chymotrypsin-like and caspase-like activity in these three different cell lysates (Figures S4A and S4B and data not shown). This pattern of β subunit proteolytic inhibition is the same as that seen in prion-infected cells and mouse brain.

Prion Infection Impairs the Proteasome by Specifically Inhibiting the Catalytic β Subunit Activity

To investigate the UPS β subunit inhibition by prions, we used specific β subunit activity probes (Berkers et al., 2005). These are cell-permeant peptide vinyl sulfone-based inhibitors that modify the catalytically active threonine residues of the β subunits, forming a covalent β-sulfonyl ether linkage. Cell lysates from ScN2aPK-1 cells were incubated with the activity probe and immunoblotted with an anti-dansyl antibody. Modification of β subunit activities (indicating a loss of activity) was clearly seen in ScN2aPK-1 cells compared to uninfected, mock-infected,

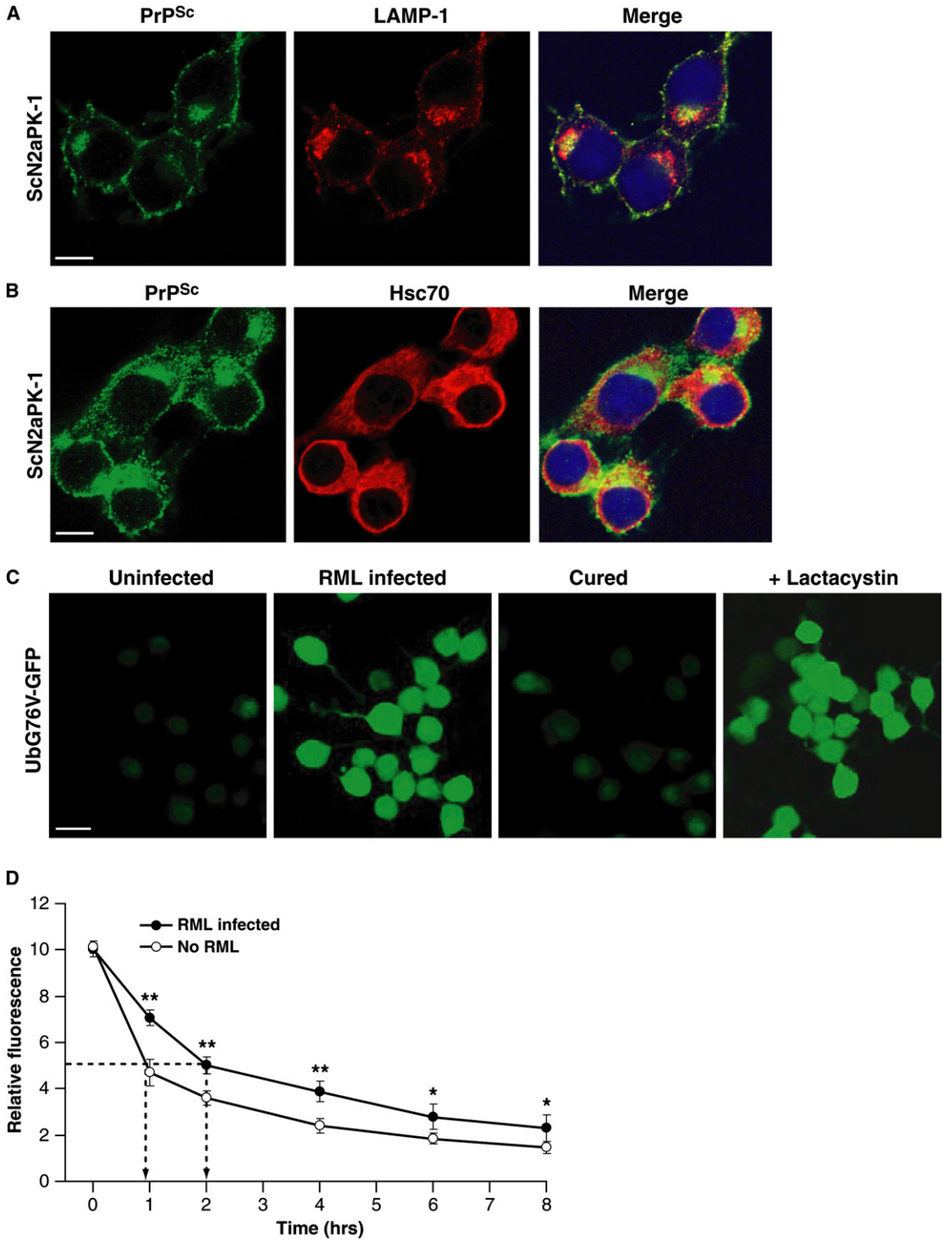

Figure 2. Prion Infection Results in Malfunction of the Intact Proteasome in Live Cells

(A) Formic acid-resistant PrP^{Sc} (ICSM18; green) in ScN2aPK-1 cells not only partially colocalizes with lysosomal-associated membrane protein-1 (LAMP-1; red) but also exists outwith this structure.

(B) A proportion of formic acid-resistant PrP^{Sc} (ICSM18; green) in ScN2aPK-1 cells colocalizes with cytosolic Hsc70 (red). PrP^{Sc} is also seen abundantly on the cell surface (green). For all panels, scale bar = 20 μm; DAPI nuclear staining (blue).

(C) Accumulation of the fluorescent GFP reporter occurs only in prion-infected Ub^{G76V}-GFP expressing N2aPK-1 cells or lactacystin-treated (50 μM) N2aPK-1 cells (positive control).

(D) ScN2aPK-1 cells took twice as long as N2aPK-1 cells to clear 50% of the accumulated Ub^{G76V}-GFP (n = 6 ± SEM).

and cured cells (Figure 3B). As these β subunit activity probes are cell permeant, we also assayed them in live GT-1 cells. Loss of β subunit activity was seen only in ScGT-1 cells (Figure S5A).

PrP^{Sc} and Aggregated Recombinant β-PrP Inhibit the Catalytic β Subunit Activity of the Proteasome

Both aggregated β-PrP and PrP^{Sc} inhibit the β subunit activities (Figure 3C), with α-PrP, aggregated α-PrP, and amyloid fibrils having no inhibitory effect (Figure 3C). We also found that reduced carboxy-methylated α-lactalbumin had no inhibitory effect (Figure 3C); this is a soluble unfolded protein molecule used in protein folding studies as a mimetic of the molten globule state (Kuwajima, 1996). PrP^{Sc} derived from RML prion-infected mouse brain also had marked inhibition on β subunit activities (Figure 3D). We also incubated cytosolic fractions from mouse CGN cultures with the different PrP species and assessed β subunit activity. β-PrP and PrP^{Sc} cause a loss of β subunit (predominantly β1 and β5) activities in CGNs (Figure 3E).

Denaturation of β-PrP and PrP^{Sc} Abolishes Their Inhibitory Effect on β Subunit Activity

Denaturation of β-PrP and PrP^{Sc} by serial freeze-boiling completely removed their inhibitory activity (Figure 3F). Inhibition of the β subunit activities is restored after denaturation, indicating that a specific conformation of the inhibitory species in β-PrP and PrP^{Sc} is necessary for inhibition of the catalytic β subunits. Nonaggregated β-PrP had no effect on proteolytic activities (Figure 3G).

β-PrP is a Highly Potent Inhibitor of 26S Proteasome β Subunit Proteolysis

To determine the potency of β-PrP in inhibiting the 26S β subunit activities, serial dilutions of aggregated β-PrP were prepared and incubated with cytosolic cell fractions prior to assaying β subunit activity. Proteolytic β subunit activity is restored to normal levels at 50 ng/ml of β-PrP (Figure S5B). To gain insight into the molar ratio of aggregated β-PrP required to inhibit the proteasome, we assayed known concentrations of pure 26S proteasome with aggregated β-PrP. The molar ratio of β-PrP that inhibits 26S proteasome is essentially stoichiometric; 100 ng final concentration (fc) 26S (1.39 nM) required 1.5 ng β-PrP (2.15nM) to inhibit (Figure 4A), 300 ng fc 26S (4.16 nM) required 3 ng β-PrP (4.3 nM) to inhibit (Figure 4B), and 900 ng fc 26S (12.49 nM) required 7.5 ng (10.75 nM) β-PrP to inhibit (Figure 4C). Data and calculations are summarized in Figure S5C. These data demonstrate that this PrP species is a highly potent inhibitor of β subunit proteolytic activity and suggest that it is likely to be a very small aggregated oligomeric PrP species that is inhibitory.

Preincubation with an Anti-Oligomer Antibody Abrogates the Inhibition of the β Subunit Activity by β-PrP and PrP^{Sc}

To investigate whether an oligomeric species of PrP was responsible for inhibition of β subunit activity, we assessed whether an anti-oligomer antibody (Kayed et al., 2003) could prevent this inhibitory effect. Preincubation of either 0.5 μg/ml aggregated β-PrP or PrP^{Sc} preparation (Figure 5Aa) with molar excess of anti-oligomer antibody (150 μg/ml) abolished their inhibitory effect on the β subunits (Figure 5Aa). The specificity of the effect was confirmed by preincubating both β-PrP and PrP^{Sc} with a rabbit polyclonal antibody against β-actin, which had no effect (Figure 5Aa). We also preincubated both PrP^{Sc} and aggregated β-PrP with the same concentration (150 μg/ml) of three anti-PrP antibodies raised against different regions of the prion protein that did not diminish the inhibitory effect of PrP^{Sc} or aggregated β-PrP (Figures 5Ab and 5Ac), confirming the specificity of the action of the anti-oligomer antibody. These data are consistent with an oligomeric PrP species in β-PrP and PrP^{Sc} inhibiting the 26S β subunit activity.

Inhibition of the Proteasome Is Specific to Conformational Isoforms of PrP

To determine if the inhibitory effect was specific to PrP^{Sc} and PrP^{Sc}-like species, we assessed the effects of other nonprion recombinant aggregated proteins on the β subunit activities. $A\beta_{1-40}$ amyloid fibrils, SOD1 mutant protein (G37R), and lysozyme amyloid fibrils were studied. The inhibitory effect on the 26S β subunits is specific to aggregated conformational isoforms of PrP as none of the other proteins assayed had any inhibitory effect (Figure 5B). Only the presence of aggregated β-PrP and PrP^{Sc} had a significant inhibitory effect on chymotrypsin-like and caspase-like activity in pure 26S proteasome (Figure 5C) and our three different cell lines (Figures S6 and S7).

Oligomeric PrP Species Inhibit the 20S Proteasome Catalytic Core, but Not via Dissociation of the 26S Proteasome

Dissociation of the 26S proteasome into the 20S core particle and 19S regulatory particle causes inhibition of proteolysis (Elsasser et al., 2005). To probe whether our data could be explained by PrP causing dissociation of the 26S proteasome and inhibiting its activity, we used native gels to assess the effect of aggregated β-PrP and PrP^{Sc} on native 26S proteasome. Native PAGE using 19S and 20S antibodies shows that aggregated β-PrP and PrP^{Sc} do not cause dissociation of the 26S proteasome (Figure 6A). This was confirmed by native gel activity staining (Figure 6B) using the fluorogenic substrate overlay for chymotrypsin activity. Both aggregated β-PrP and PrP^{Sc} significantly inhibit chymotrypsin activity in native 26S proteasome compared to untreated 26S (Figure 6B). Coomassie staining confirmed equal protein loading (Figure S8A). Native PAGE of ScGT-1 cells and prion-infected mouse brain demonstrates that there is no dissociation of the 26S proteasome (Figure S8B).

We tested whether oligomeric PrP species could affect the 20S proteasome core particle independent of the 19S regulatory cap. We substituted the 19S regulatory particle with the PA28 activator (Whitby et al., 2000), which activates the proteasome core particle but does not mediate

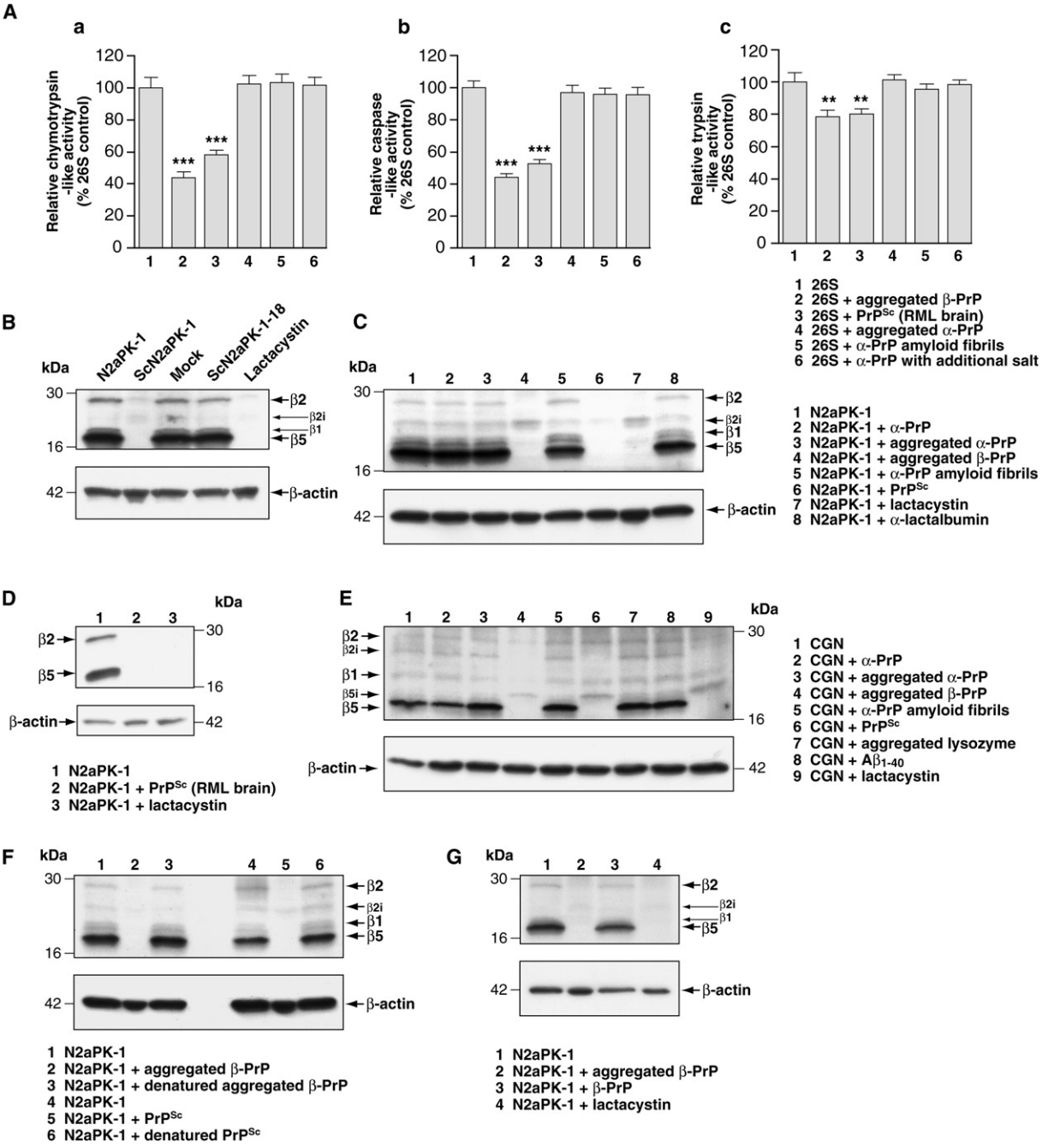

Figure 3. PrP^{Sc} and Aggregated β-PrP Inhibit the Proteolytic Activities of the 26S Proteasome

(A) Only aggregated β-PrP and PrP^{Sc} decrease proteolytic activities in pure 26S proteasome. Data are mean ± SEM with n = 10.

(B) N2aPK-1 cell lysates were incubated with the β subunit activity probe and immunoblotted. Only prion infection of N2aPK-1 cells resulted in a loss of proteolytic β subunit activities.

(C) Only aggregated β-PrP (lane 4), PrP^{Sc} (lane 6), or 50 μM lactacystin (lane 7) resulted in a loss of β subunit activity in N2aPK-1 cell lysates.

(D) PrP^{Sc} from RML brain incubated with N2aPK-1 cell lysates resulted in a loss of β subunit activity.

(E) Aggregated β-PrP (lane 4), PrP^{Sc} (lane 6), or 50 μM lactacystin (lane 9) resulted in a loss of β1 and β5 subunit activity in lysates from primary cerebellar granule neurons (CGNs).

(F) Complete denaturation of aggregated β-PrP and PrP^{Sc} restored β subunit catalytic activities (lanes 3 and 6, respectively) to normal (lanes 1 and 4).

(G) Only β-PrP in an aggregated state inhibited β subunit activities (lane 2) in N2aPK-1 cell lysates.

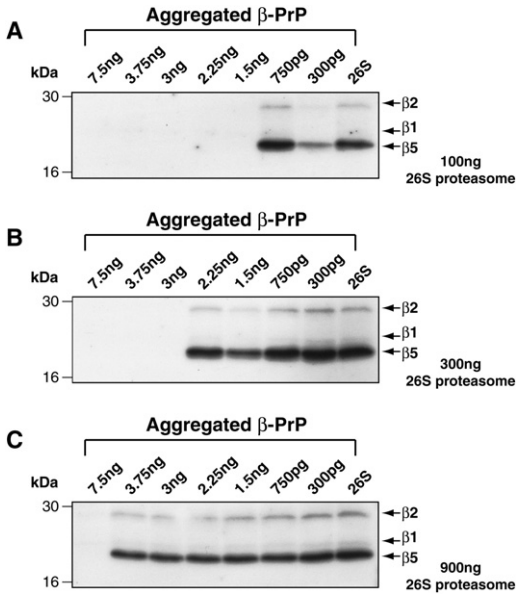

Figure 4. β-PrP Is a Highly Potent Inhibitor of 26S Proteasome β Subunit Proteolysis

To determine potency of aggregated β-PrP in inhibiting the 26S proteolytic activity, serial dilutions of aggregated β-PrP were preincubated with three different concentrations of 26S proteasome before incubation with the β subunit activity probe. (A) 100 ng final concentration of 26S proteasome required 1.5 ng aggregated β-PrP to inhibit β subunit proteolysis, (B) 300 ng final concentration of 26S proteasome required 3 ng aggregated β-PrP to inhibit β subunit proteolysis, and (C) 900 ng final concentration of 26S proteasome required 7.5 ng aggregated β-PrP to inhibit β subunit proteolysis.

ubiquitin-dependent proteolysis and many other activities mediated by the 19S regulator particle (Voges et al., 1999). Assaying PA28-activated 20S showed that aggregated β-PrP and PrP^{Sc} significantly inhibited chymotrypsin-like (Figure 6Ca) and caspase-like activity (Figure 6Cb) with a lesser effect on trypsin activity (Figure 6Cc). This again is the same pattern of inhibition as seen with pure 26S proteasome (Figure 3A), but with a less profound inhibitory effect. These data strongly suggest that the oligomeric inhibitory PrP species exert their effect directly on the 20S particle independent of the 19S complex.

Prion Infection Causes Specific Inhibition of the UPS in GFP-Proteasome Reporter Transgenic Mice In Vivo

To assess whether UPS impairment also occurred in prion-mediated neurodegeneration in vivo, we studied a transgenic mouse model that allows the functional status of the UPS to be monitored (Lindsten et al., 2003). These mice express the Ub^{G76V}-GFP reporter under the control of the CMV-immediate early enhancer and the chicken β-actin promoter with constitutive and ubiquitous expression throughout the body, including the brain. Accumulation of Ub^{G76V}-GFP occurred only in the 22L prion-infected transgenic mouse brains and was seen in regions of the brain with the most intense neuropathology, consisting of spongiosis, gliosis, and PrP^{Sc} deposition (Figure 7A). Similar results were obtained with the two available reporter mouse strains established from different founders (Lindsten et al., 2003). Quantitative PCR confirmed that the accumulation of Ub^{G76V}-GFP was not due to transcriptional upregulation (Figure S9). There was no Ub^{G76V}-GFP accumulation in mice inoculated with normal brain or in 22L prion-infected nontransgenic littermates (Figure 7A). In the brains of the 22L prion-infected Ub^{G76V}-GFP mice, we found accumulation of intraneuronal cytoplasmic, granular, ubiquitinated deposits (Figure 7B). These were occasionally observed in the control mice but only at very low levels (Figure 7B). The expression of the Ub^{G76V}-GFP transgene appeared to have no detectable effect on the deposition of ubiquitinated proteins (Figure 7B). These data suggest that prion disease in vivo is associated with UPS dysfunction and support the in vitro studies indicating that proteasome function is directly compromised by the presence of PrP^{Sc} or its synthetic mimetic β-PrP.

DISCUSSION

While prion infection causes widespread neuronal loss in the brain, the molecular basis of prion neurotoxicity is unknown. Neurodegeneration cannot be explained by a loss of functional PrP^{C}, as its depletion does not trigger any gross pathology. The alternative explanation, that PrP^{Sc} itself is neurotoxic, does not adequately describe findings where neurons can be in close proximity to PrP^{Sc} deposits without suffering deleterious effects, providing those cells do not express cell-surface PrP^{C}. It has been suggested that PrP^{Sc} interacts with cell-surface PrP^{C}, which results in apoptosis through aberrant signaling cascades (Solforosi et al., 2004). An alternative explanation is that intracellular accumulation of disease-associated PrP is required for cytotoxicity. Here, we present both in vitro and in vivo experimental evidence for a potential neurotoxic mechanism mediated by specific misfolded forms of PrP that would explain the lack of direct toxicity from extracellular PrP^{Sc}. We also demonstrate in vivo functional impairment of the UPS in a neurodegenerative disease. We have established that oligomeric nonnative forms of PrP inhibit the activity of the catalytic β subunits of the 26S proteasome and that this occurs at stoichiometric concentrations.

Using fluorogenic peptide assays and β subunit activity probes, we demonstrated in two prion-infected neuronal cell lines that the presence of misfolded PrP significantly inhibits the chymotrypsin-like and caspase-like activities; this finding was mirrored in RML prion-infected CD-1 mouse brain. This supports previous work where impairment of these activities has been shown in mouse brain infected with a different prion strain (Kang et al., 2004). Inactivation of the chymotrypsin-like sites causes significant inhibition of protein degradation (Chen and Hochstrasser,

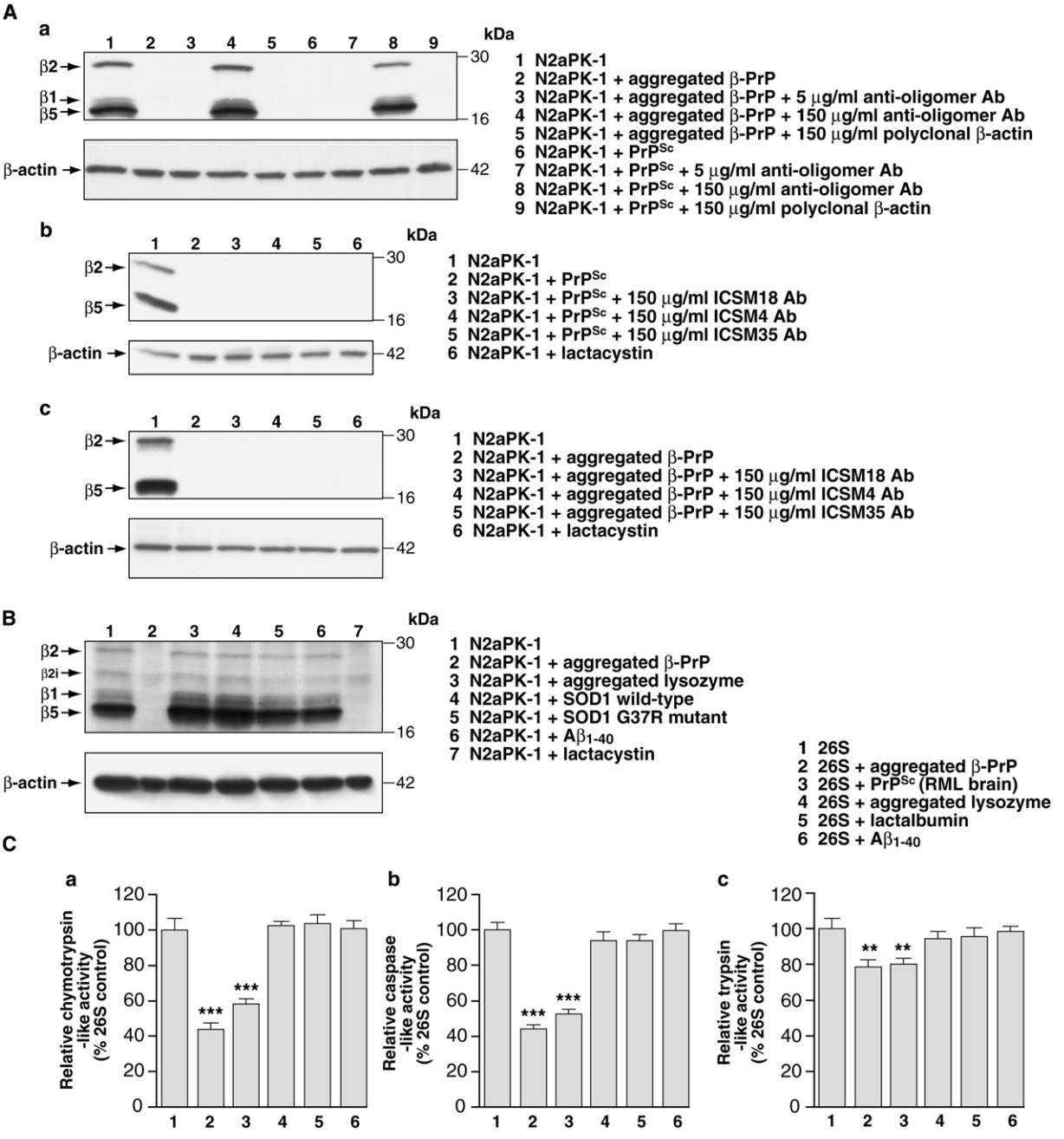

Figure 5. Inhibition of the Proteolytic Activities of the Proteasome Is Specific to Conformational Isoforms of PrP and Is Abrogated by Preincubation with an Anti-Oligomer Antibody

(Aa) Preincubating aggregated β-PrP (lane 4) or PrP^{Sc} (lane 8) with high concentrations (150 μg/ml) of anti-oligomer antibody abolished their inhibitory effect on β subunit activities in N2aPK-1 cell lysates. An unrelated protein (β-actin) had no effect on preventing inhibitory action of β-PrP (lane 5) or PrP^{Sc} (lane 9). (Ab) Preincubating PrP^{Sc} or (Ac) aggregated β-PrP with high concentrations (150 μg/ml) of mouse monoclonal anti-PrP antibodies (ICSM 4, 18, or 35) raised against different regions of PrP did not abolish their inhibitory effect on β subunit activities in N2aPK-1 cells.

(B) Nonprion recombinant aggregated protein species had no effect on 26S proteasome β subunit activities in N2aPK-1 cell lysates using the β subunit activity probe.

(C) Nonprion recombinant protein species had no effect on proteolytic activities of pure 26S proteasome. Data are mean ± SEM with n = 10.

1996). However, this alone is not enough to halt protein breakdown, and either the trypsin-like or caspase-like activities must also be compromised to achieve this effect (Kisselev et al., 2006)—an observation in close agreement with our findings. Our data also demonstrated that the level of inhibition observed resulted in functional

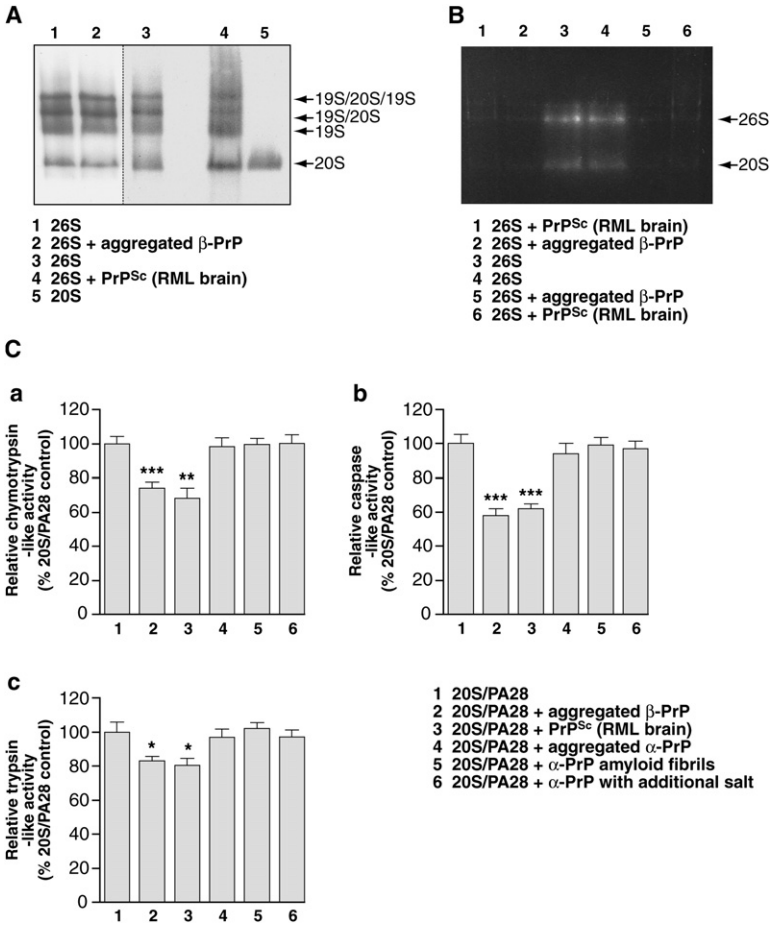

Figure 6. Oligomeric PrP Species Inhibit the 20S Proteasome Catalytic Core, but Not via Dissociation of the 26S Proteasome

(A) Native gel immunoblot using 19S and 20S antibodies demonstrated aggregated β-PrP and PrP^{Sc} do not cause dissociation of the 26S proteasome into its 19S and 20S components.

(B) Pure 26S proteasome incubated with aggregated β-PrP or PrP^{Sc} was run on a native gel and stained with a fluorogenic substrate to detect chymotrypsin-like activity. The native-gel activity stain shows that aggregated β-PrP (lanes 2 and 5) and PrP^{Sc} (lanes 1 and 6) significantly inhibited chymotrypsin-like activity in intact pure 26S proteasome.

(C) Only aggregated β-PrP and PrP^{Sc}, but not aggregated conformational isoforms of PrP, decrease proteolytic activities of PA28-activated 20S proteasome. Data are mean ± SEM with n = 10.

impairment of the UPS in live cells with significant accumulation of the proteasome reporter substrate Ub^{G76V}-GFP. This was abrogated by curing the cells of prion infection, demonstrating a direct link between prion infection and UPS impairment in live cells. These cells only propagate low levels of PrP^{Sc}, which is relatively sensitive to PK digestion, and by inference clearance. This is likely to be a unique feature that allows them to propagate prions without obvious cytotoxicity (Weissmann, 2004), and thus, they are able to tolerate this level of UPS dysfunction. When their UPS becomes further impaired they rapidly undergo apoptosis (Kristiansen et al., 2005).

In an in vitro assay system we developed, we show that PrP^{Sc} and aggregated β-PrP, but not recombinant PrP^{C} or PrP amyloid fibrils, inhibited proteolysis by the 26S proteasome. The sequence and conformational specificity of the inhibitory effect was tested by measuring the effects of $A\beta_{1-40}$ amyloid fibrils, SOD1 G37R mutant protein, aggregated lysozyme, and α-lactalbumin, all of which had no effect. Moreover, conformational disruption of PrP^{Sc} and β-PrP abolished their inhibitory properties, demonstrating that the effect depends on a specific conformation and aggregation state.

Dose-response analysis showed that inhibition of the catalytic activity of the 26S proteasome by β-PrP occurred at a low stoichiometry. However, because the proportion of active 26S proteasome complexes in the preparation is unknown, it is impossible to determine the true molecular stoichiometry for the inhibited proteasome species. We have previously argued, based on observations in subclinical models of prion infection, that prion neurotoxicity may relate not to PrP^{Sc} (or prions) but to critical levels of a toxic oligomeric species produced during prion propagation (designated PrP^{L} with L for lethal) (Hill and Collinge, 2003). Our current data are supportive of this, and it is also apparent from these data that the affinity of PrP^{L} for the proteasome is extremely high. To investigate this further, we used an antibody that reacts with oligomeric, but not monomeric or fibrillar, forms of amyloidogenic proteins. Preincubation with this antibody completely abolished any inhibitory effect on the catalytic β subunits, suggesting that an oligomeric PrP species may be responsible for the inhibition of the 26S proteasome.

Together, our data support an inhibitory effect of oligomeric PrP species on the 20S complex itself, and the differential inhibitory effect of prions on the caspase-like (β1) and chymotrypsin-like (β5) proteolytic activities versus the minor effect on the trypsin-like activity (β2) can be explained by two possible mechanisms. The first is that oligomeric PrP species have a direct inhibitory effect on the β1

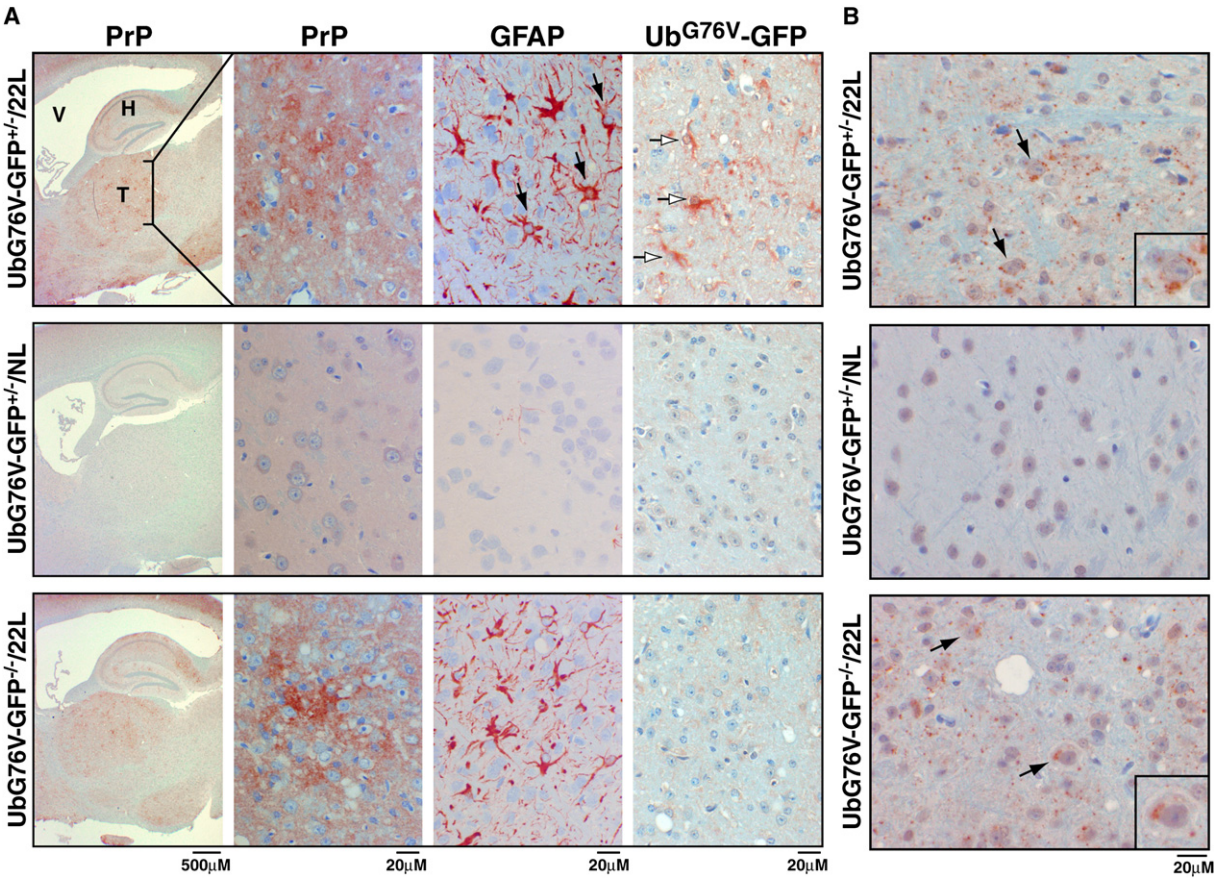

Figure 7. Prion Infection Causes Specific Inhibition of the UPS in GFP-Proteasome Reporter Transgenic Mice with Accumulation of Ubiquitin Deposits

(A) Immunohistochemical studies of UbG76V-GFP$^{+/-}$ transgenic mice inoculated intracerebrally with the 22L strain of mouse scrapie (UbG76V-GFP$^{+/-}$/22L) (top) or normal brain homogenate (UbG76V-GFP $^{+/-}$/NL) (middle) and UbG76V-GFP$^{-/-}$ inoculated with 22L (UbG76V-GFP$^{-/-}$/22L) (bottom). Left panels show low-power views of saggital sections through the hippocampus (H), third ventricle (V), and thalamus (T) stained with anti-PrP antiserum R30. Other panels show high-power views of the thalamus stained for PrP, GFAP, and Ub^{G76V}-GFP. The 22L-inoculated mice exhibited primarily diffuse staining for PrP and extensive astrocytosis (black arrows point to hypertrophic astrocytes). Collections of Ub^{G76V}-GFP + cells were seen in the 22L inoculated UbG76V-GFP$^{+/-}$ mice (open arrows). The specificity of the anti-Ub^{G76V}-GFP antiserum is demonstrated by the lack of staining of these cells in the 22L inoculated UbG76V-GFP$^{-/-}$ mice.

(B) Immunohistochemical staining for ubiquitin in sections of thalamus from UbG76V-GFP$^{+/-}$ mice inoculated with 22L prion strain or normal brain homogenate. Granular deposits of ubiquitin are seen scattered throughout the sections of the 22L-infected brain but were rarely observed in the control. Arrows point to large neuron-like cells containing ubiquitin deposits that exhibit a perinuclear localization. The lower panel of a UbG76V-GFP$^{-/-}$ inoculated with 22L demonstrates that the expression of the transgene appeared to have no effect on the deposition of ubiquitinated proteins. The substrate for all antisera was amino-ethyl-carbazol yielding a red product. Sections were counterstained with hematoxylin.

and β5 proteolytic active sites of the 20S core. However, the diameter of the gated channel is ~2 nm (Pickart and Cohen, 2004), and if the inhibitory PrP species is an oligomer, it cannot traverse the gate intact and enter the catalytic chamber. The only possibility of direct inhibition is that the PrP unfolds and threads into the chamber. The second mechanism is that prions inhibit gate opening of the 20S proteasome. Entry of substrates into the catalytic chamber of the 20S is regulated by opening of the gated channel, which is normally held closed by the N-terminal tails of the outer α ring subunits (Groll et al., 2000; Whitby et al., 2000). Studies of gate opening with addition of hydrophobic peptides, use of PA28 activator, or gate deletion (which all accelerate substrate entry) stimulate cleavage at the chymotrypsin-like and caspase-like sites by enhancing their V_{max} but do not stimulate the slower cleavage at the trypsin-like site (Prof. A. Goldberg, Harvard University, personal communication; Kisselev et al., 2002). Therefore, an inhibitory effect of prions on gate opening of the 20S proteasome would have a more severe inhibitory effect on the chymotrypsin-like and caspase-like activities rather than the trypsin-like site—an effect we clearly see in our data. The levels of proteasome inhibition observed (>50% loss in each caspase-like and chymotrypsin-like activity) are likely to have serious consequences for neuronal viability, as inhibition of these two

of the 20S catalytic sites have additive effects in reducing protein degradation (Kisselev et al., 2006). The degradative capacity of the UPS is also known to decline during the aging process (Lee et al., 2000), and combined with the effects of neuronal stress in the brain, this will further incapacitate UPS function, resulting in neuronal dysfunction (Sherman and Goldberg, 2001).

Therefore to ascertain whether our in vitro data had in vivo relevance, and importantly whether prions were exerting a similar inhibitory effect on the UPS in vivo, we studied proteasome reporter mice. These mice enable in vivo testing of the role of the UPS in neurodegeneration; they have been used to demonstrate that proteasome impairment does not contribute to pathogenesis in an SCA7 mouse model (Bowman et al., 2005). Their data also show that neuronal apoptosis per se does not cause accumulation of the reporter, which is only seen when there is significant UPS dysfunction. Accumulation of the Ub^{G76V}-GFP reporter occurred only in our prion-infected mice brains. Intracellular accumulation of the GFP reporter was associated with neuronal loss and PrP^{Sc} deposition, indicating a relationship between UPS dysfunction and prion-mediated neurodegeneration in vivo. In the brains of prion-infected GFP-reporter mice, we also found accumulation of intracellular cytosolic granular ubiquitinated deposits, which are likely to represent cytosolic ubiquitinated-protein conjugates that accumulate as they are not degraded by the failing proteasome. Interestingly, similar ubiquitin-protein conjugates within neurons were reported in the brains of prion-infected mice (Lowe et al., 1992). They found that these intracellular ubiquitinated deposits were seen early in the course of the incubation time when mice were presymptomatic, and increased with disease progression. They noted that the pathological accumulation of the intracellular ubiquitin-protein structures corresponded temporally with the earliest detection of PrP^{Sc} (Lowe et al., 1992). These observations can now be explained by our data. Although proteasome impairment has been suggested to be important in neurodegenerative diseases from many in vitro studies and assays of postmortem brain material, it has not yet been directly demonstrated in vivo.

Together, our data support the view that prion protein neurotoxicity may be mediated through toxic oligomers. There is growing evidence in protein misfolding disorders that smaller intermediate oligomeric protein species may be biologically more active than larger amyloid fibrils (Caughey and Lansbury, 2003). In studies of prion infectivity, nonfibrillar prion particles with masses equivalent to 14–28 PrP molecules are the most efficient initiators of prion disease (Silveira et al., 2005). Our current data also support a cytosolic localization for a small proportion of PrP^{Sc} in prion-infected neuronal cells, in line with our previous data demonstrating toxic cytosolic PrP^{Sc} aggresomes (Kristiansen et al., 2005). Granular deposits of disease-related PrP have been reported in the cell body of neurons in CJD brain, suggesting the occurrence of intraneuronal prion aggregates (Kovacs et al., 2005). The very high-affinity, stoichiometric inhibition of the proteasome we demonstrate means that only a small amount of PrP^{Sc} molecules in the cytosol may be necessary to have a toxic effect. How PrP^{Sc} oligomers traffic inside neurons and enter the cytosol and result in UPS inhibition is not known. Possible sites of entry include retrotranslocation from the ER (Ma and Lindquist, 2001; Yedidia et al., 2001) or via endolysosomal membrane destabilization and leakage into the cytosol, as described for diphtheria toxin and other A-B toxins (Sandvig and van Deurs, 2002) and $A\beta_{1-42}$ (Ji et al., 2006). It is also possible that PrP^{Sc} accumulation in the endolysosomal system causes dysfunction of this pathway, resulting indirectly in an increased burden on the UPS.

Previous studies have suggested that intracellular neuronal propagation of pathogenic PrP appears important for neurotoxicity (Mallucci et al., 2003; Chesebro et al., 2005; Brandner et al., 1996). Here, we have shown results that suggest an intracellular mechanism whereby toxic prion oligomers impair the proteasome in vivo by inhibiting the catalytic β subunits. The pathogenesis of prion disease is likely to be multifactorial, but the potent inhibition of the proteasome by pathogenic PrP is likely to result in neuronal perturbation and contribute to the widespread neuronal loss. Our data also explain how cytosolic PrP^{C} may accumulate in prion disease, with UPS inhibition leading to the cytosolic accumulation of PrP^{C} destined for ER-associated degradation (Ma and Lindquist, 2002). Impairment of the UPS leads to cellular dysfunction and apoptosis through many different mechanisms, as the UPS is also involved in transcriptional regulation, cell-cycle control, and control of apoptosis (Goldberg, 2003). The key feature of prion disease, autocatalytic conversion of PrP^{C} to PrP^{Sc}, will form a positive feedback loop by inhibiting the UPS, thereby reducing the rate of clearance of PrP^{Sc} and thus stimulating the formation of more PrP^{Sc} until the levels of proteasome function are too low for cell survival. A key question that arises is whether our findings are relevant to other neurodegenerative diseases associated with protein misfolding or a unique property specific to prion diseases.

EXPERIMENTAL PROCEDURES

Cell Culture and Prion Infection

GT-1 and N2aPK-1 mouse neuronal cells were exposed to homogenates from RML prion-infected or uninfected CD-1 mouse brain. Cells were subcultured, tested for the presence of newly generated PrP^{Sc}, and cured of prion infection (Kristiansen et al., 2005).

SDS-PAGE and Immunoblot Analysis

Cells and brain tissue were homogenized, proteinase K digested, electrophoresed, and immunoblotted (Kristiansen et al., 2005). For assaying proteasome subunits, immunoblotting was performed (see Supplemental Experimental Procedures).

Preparation of Recombinant Protein Species

Recombinant murine PrP^{23-231} in either the oxidized α form or the reduced β form was prepared (Jackson et al., 1999a, 1999b). Proteins were buffer exchanged into PBS. Monomeric α-PrP was aggregated by thermal denaturation (70°C for 10 min). Aggregated β-PrP was produced by increasing the salt concentration to 270 mM and was allowed

to proceed for 1 hr. Aggregated β-PrP was denatured by ten cycles of freeze/boiling at 100°C. α-PrP amyloid fibrils were prepared as described (Baskakov et al., 2002) and visualized by EM. Lysozyme was aggregated by the addition of 50 mM DTT for 1 hr. Amyloid-β_{1-40} (Sigma) was aggregated immediately by the addition of water and assayed at a final concentration of 100 μg/ml. SOD1 wild-type and SOD1 mutant (G37R) recombinant proteins were prepared in PBS, and α-lactalbumin (Sigma) was prepared in water. All proteins were assayed at a final concentration of 1 mg/ml unless specified.

Enrichment of PrP^{Sc} from ScGT-1 Cells

After 24 hr of 1 μM lactacystin treatment, ten 10 cm plates of ScGT-1 or ScN2aPK-1 cells were harvested, washed in ice-cold PBS, freeze-thawed three times, and centrifuged at 1000 × g for 10 min at 4°C to remove cellular debris. The supernatant was adjusted with an equal volume of 2× lysis buffer (100 mM Tris [pH 7.4[, 300 mM NaCl, 4 mM EDTA, 1% Triton X-100, and 1% deoxycholate) followed by incubation with benzonase (50 U/ml) for 20 min at 4°C. Lysates were incubated with PK at 1 μg/mg protein (37°C, 90 min), followed by treatment with AEBSF (8 mM) for 10 min at 37°C. The whole mixture was centrifuged at 100,000 × g for 45 min, sonicated in PBS to dissociate the material, and the presence of PrP^{Sc} was confirmed by immunoblotting. The pellet of PrP^{Sc} was assayed at a final concentration of 1 mg/ml. PrP^{Sc} was denatured as described for β-PrP above. For enrichment of PrP^{Sc} from RML-infected mouse brain, a modification of the above protocol was used (see Supplemental Experimental Procedures).

Probing Proteasome β Subunit Activity Using Activity Probes

To prepare lysates for proteasome activity probe assays, N2aPK-1 cells or CGNs were pelleted and lysed in fresh lysis buffer (50 mM Tris [pH 7.4], 5 mM $MgCl_2$, 2 mM ATP, 250 mM sucrose, and 1 mM DTT) as described (Berkers et al., 2005). One-hundred micrograms of protein was incubated with 1 μM dansylAhx3L3VS probe for 1 hr at 37°C before assaying by immunoblotting. For live-cell experiments, GT-1 cells were incubated with 10 μM probe in culture for 1 hr at 37°C before pelleting and lysing as above. For assays with 26S proteasome, either 100, 300, or 900 ng 26S proteasome (BIOMOL) was incubated with 1 μM probe for 1 hr at 37°C before assaying by immunoblotting (see Supplemental Experimental Procedures). All recombinant proteins were incubated for 1 hr at 37°C in the presence of 2 mM ATP with 100 μg cell lysates, before a further 1 hr incubation at 37°C with 1 μM probe.

Assaying Proteasome Activity with Fluorogenic Substrates

Assays were performed as described (Berkers et al., 2005; Dantuma et al., 2000; Kisselev and Goldberg, 2005). Ten micrograms of protein from cell lysates was added to 100 μl reaction buffer containing 50 mM Tris-HCl (pH 7.4), 5 mM $MgCl_2$, 1 mM DTT, 2 mM ATP, and 100 μM Suc-LLVY-AMC (BIOMOL), Boc-LRR-AMC (BIOMOL), or Ac-nLPnLD-AMC (BACHEM). Fluorescence was measured every minute for 30 min at 37°C by using a TECAN 96-well plate reader ($\lambda_{ex}/\lambda_{em}$ = 360/440nm). Nonspecific hydrolysis was assessed by preincubation of cells for 30 min at 37°C with 50 μM epoxomicin and subtracted from each measurement. Lysates of 10% brain homogenate were prepared in homogenisation buffer, freeze-thawed three times, and sonicated before digestion with benzonase (50 U/ml on ice, 15 min) and centrifugation at 16,000 × g for 10 min at 4°C. A 10 μg cytosolic brain fraction was assayed as described above. For pure proteasome assays, 10 ng of pure 26S proteasome or 10 ng (0.014 pmol) 20S proteasome (BIOMOL) activated with 32 ng (0.06 pmol) of human PA28α/β activator (BIOMOL) was added to 100 μl reaction buffer and assayed as described above. All recombinant proteins were incubated for 1 hr at 37°C in the presence of 2 mM ATP with 10 μg cell lysates, 10 ng 26S proteasome, or 10 ng of PA28-activated 20S proteasome, before incubation with fluorogenic substrates in reaction buffer as described above (see Supplemental Experimental Procedures).

Live-Cell GFP-Proteasome Reporter Assays

Transfection of the Ub^{G76V}-GFP construct (Dantuma et al., 2000) into N2aPK-1 cells was performed with Genejammer (Stratagene). Stable cell lines were generated by selection in 600 μg/ml gentamicin (G418). Fluorescence half-life was measured in N2aPK-1-transfected cells by using the FL-1 channel of FACSCalibur (BD Biosciences). For inhibition of protein synthesis, 20 μg/ml cycloheximide was added for 30 min at 37°C prior to fluorescent half-life measurement. For visualization of GFP accumulation, Ub^{G76V}-GFP-transfected N2aPK-1 cells were grown on coverslips, fixed in 4% PFA, permeabilized in ice-cold methanol, and blocked in 10% normal goat serum before visualization by using the confocal microscope (Zeiss) (see Supplemental Experimental Procedures).

Confocal Microscopy and Immunofluorescence

These were performed as described (Kristiansen et al., 2005). Antibody details are in the Supplemental Experimental Procedures.

Incubation of β-PrP and PrP^{Sc} with Oligomer-Specific and Anti-PrP Antibodies

Either 500 ng/ml aggregated β-PrP or 500 ng/ml PrP^{Sc} was incubated (RT, 1 hr) with 5 μg/ml or 150 μg/ml of a rabbit polyclonal antibody raised against oligomeric protein species (Kayed et al., 2003) or 150 μg/ml of mouse monoclonal anti-PrP antibodies (ICSM 4, 18, or 35). These mixtures were incubated with 100 μg of cytosolic fraction from cell lysates (1 hr, 37°C) with 2 mM ATP on a shaker before addition of 1 μM probe (1 hr, 37°C), and analysis by immunoblotting was as described above. For controls, aggregated β-PrP or PrP^{Sc} was incubated (1 hr, 37°C) with mouse monoclonal (Sigma; 150 μg/ml) or rabbit polyclonal β-actin antibodies (Abcam; 150 μg/ml) before incubation with 100 μg cell lysates.

Native Gel Fluorogenic Activity Stain and Immunoblotting

Native gel chymotrypsin activity stain and native gel immunoblotting using anti-19S and 20S antibodies were performed as described (Elsasser et al., 2005) with minor modifications using the Invitrogen NativePAGE Novex Bis-Tris 3%–12% Gel system (Invitrogen) (see Supplemental Experimental Procedures).

Prion Infection of GFP-Proteasome Reporter Mice

Two lines of transgenic UPS-reporter mice, Ub^{G76V}-GFP/1 and 2 (Lindsten et al., 2003), were studied. Mice heterozygous for the transgene were bred to C57BL/6 mice, and the offspring were inoculated intracerebrally with 50 μl 1% w/v brain homogenates from 22L infected or uninoculated mice. The mice were followed by visual observation and sacrificed at the time when clear signs of clinical disease were manifested (i.e., rocking gait, ruffled fur, and immobility). Mice were perfused with PBS through the left ventricle, and the brains removed and processed either for histology or for RNA isolation and real-time rtPCR (Dimcheff et al., 2003).

Immunohistochemistry

Paraffin sections to be stained for GFP, ubiquitin, and PrP were first subjected to pretreatment at 120°C for 20 min in citrate buffer (pH 6). Sections for GFAP staining were not pretreated. Antibody details are in the Supplemental Experimental Procedures. Staining for all but GFP was performed as described (Dimcheff et al., 2003) by using either biotinylated secondary antisera followed by horseradish peroxidase-conjugated streptavidin and amino-ethyl-carbazol as substrate. GFP was detected by using diaminobenzidine as substrate. A total of 20 UbG76V-$GFP^{+/-}$ and 11 UbG76V-$GFP^{-/-}$ scrapie-inoculated mice and ten UbG76V-$GFP^{+/-}$ and two UbG76V-$GFP^{-/-}$ mice inoculated with normal brain homogenates were examined microscopically. No differences between line 1 and line 2 mice were detected, and data presented are from line 1 mice.

Statistical Analysis

Data were analyzed by two-tailed Student's t test, and significance was expressed as follows: *$p < 0.01$, **$p < 0.001$, and ***$p < 0.0001$ unless otherwise specified. Most assays represented ten independent experiments from ten different cell lysate preparations or five independent brain lysates from different mice. For all graphs, bars represent mean ± SEM unless specified.

Supplemental Data

Supplemental Data include Supplemental Experimental Procedures, Supplemental References, and nine figures and can be found with this article online at http://www.molecule.org/cgi/content/full/26/2/175/DC1/.

ACKNOWLEDGMENTS

We thank J. Wadsworth, S. Brandner, and A.L. Goldberg for experimental suggestions and advice; G. Bates for helpful comments on the manuscript; Dr. Glabe for the anti-oligomer antibody; R. Young for graphics; and S. Jones, H. Tattum, R. Chia, A. Ward, F. McAtee, C. Favara, and D. Long for technical help. This work was funded by the Medical Research Council and UK Department of Health and supported in part by the Intramural Research Program of the NIH, NIAID. S.J.T. is a UK DH National Clinician Scientist. N.P.D. is supported by the Swedish Research Council. P.D. is the recipient of a Brain Research Trust Studentship.

Received: April 4, 2006
Revised: January 8, 2007
Accepted: April 3, 2007
Published: April 26, 2007

REFERENCES

Baskakov, I.V., Legname, G., Baldwin, M.A., Prusiner, S.B., and Cohen, F.E. (2002). Pathway complexity of prion protein assembly into amyloid. J. Biol. Chem. *277*, 21140–21148.

Bence, N.F., Sampat, R.M., and Kopito, R.R. (2001). Impairment of the UPS by protein aggregation. Science *292*, 1552–1555.

Berkers, C.R., Verdoes, M., Lichtman, E., Fiebiger, E., Kessler, B.M., Anderson, K.C., Ploegh, H.L., Ovaa, H., and Galardy, P.J. (2005). Activity probe for in vivo profiling of the specificity of proteasome inhibitor bortezomib. Nat. Methods. *2*, 357–362.

Bett, J.S., Goellner, G.M., Woodman, B., Pratt, G., Rechsteiner, M., and Bates, G.P. (2006). Proteasome impairment does not contribute to pathogenesis in R6/2 HD mice: exclusion of proteasome activator REGgamma as a therapeutic target. Hum. Mol. Genet. *15*, 33–44.

Bowman, A.B., Yoo, S.Y., Dantuma, N.P., and Zoghbi, H.Y. (2005). Neuronal dysfunction in a polyglutamine disease model occurs in the absence of UPS impairment and inversely correlates with the degree of nuclear inclusion formation. Hum. Mol. Genet. *14*, 679–691.

Brandner, S., Isenmann, S., Raeber, A., Fischer, M., Sailer, A., Kobayashi, Y., Marino, S., Weissmann, C., and Aguzzi, A. (1996). Normal host prion protein necessary for scrapie-induced neurotoxicity. Nature *379*, 339–343.

Bueler, H., Aguzzi, A., Sailer, A., Greiner, R.A., Autenried, P., Aguet, M., and Weissmann, C. (1993). Mice devoid of PrP are resistant to scrapie. Cell *73*, 1339–1347.

Caughey, B., and Lansbury, P.T., Jr. (2003). Protofibrils, pores, fibrils, and neurodegeneration: separating the responsible protein aggregates from the innocent bystanders. Annu. Rev. Neurosci. *26*, 267–298.

Caughey, B., and Baron, G.S. (2006). Prions and their partners in crime. Nature *443*, 803–810.

Chen, P., and Hochstrasser, M. (1996). Autocatalytic subunit processing couples active site formation in the 20S proteasome to completion of assembly. Cell *86*, 961–972.

Chesebro, B., Trifilo, M., Race, R., Meade-White, K., Teng, C., LaCasse, R., Raymond, L., Favara, C., Baron, G., Priola, S., et al. (2005). Anchorless prion protein results in infectious amyloid disease without clinical scrapie. Science *308*, 1435–1439.

Ciechanover, A., and Brundin, P. (2003). The UPS in neurodegenerative diseases. Sometimes the chicken, sometimes the egg. Neuron *40*, 427–446.

Dantuma, N.P., Lindsten, K., Glas, R., Jellne, M., and Masucci, M.G. (2000). Short-lived green fluorescent proteins for quantifying ubiquitin/proteasome-dependent proteolysis in living cells. Nat. Biotechnol. *18*, 538–543.

Dimcheff, D.E., Askovic, S., Baker, A.H., Johnson-Fowler, C., and Portis, J.L. (2003). ER stress is a determinant of retrovirus-induced spongiform neurodegeneration. J. Virol. *77*, 12617–12629.

Elsasser, S., Schmidt, M., and Finley, D. (2005). Characterization of the proteasome using native gel electrophoresis. Methods Enzymol. *398*, 353–363.

Forloni, G., Angeretti, N., Chiesa, R., Monzani, E., Salmona, M., Bugiani, O., and Tagliavini, F. (1993). Neurotoxicity of a prion protein fragment. Nature *362*, 543–546.

Goldberg, A.L. (2003). Protein degradation and protection against misfolded or damaged proteins. Nature *426*, 895–899.

Groll, M., Bajorek, M., Kohler, A., Moroder, L., Rubin, D.M., Huber, R., Glickman, M.H., and Finley, D. (2000). A gated channel into the proteasome core particle. Nat. Struct. Biol. *7*, 1062–1067.

Harris, D.A., and True, H.L. (2006). New insights into prion structure and toxicity. Neuron *50*, 353–357.

Hegde, R.S., Mastrianni, J.A., Scott, M.R., DeFea, K.A., Tremblay, P., Torchia, M., DeArmond, S.J., Prusiner, S.B., and Lingappa, V.R. (1998). A transmembrane form of the prion protein in neurodegenerative disease. Science *279*, 827–834.

Hershko, A., and Ciechanover, A. (1998). The ubiquitin system. Annu. Rev. Biochem. *67*, 425–479.

Hetz, C., Russelakis-Carneiro, M., Maundrell, K., Castilla, J., and Soto, C. (2003). Caspase-12 and ER stress mediate neurotoxicity of pathological prion protein. EMBO J. *22*, 5435–5445.

Hill, A.F., and Collinge, J. (2003). Subclinical prion infection. Trends Microbiol. *11*, 578–584.

Jackson, G.S., Hill, A.F., Joseph, C., Hosszu, L.L.P., Clarke, A.R., and Collinge, J. (1999a). Multiple folding pathways for heterologously expressed human prion protein. Biochim. Biophys. Acta *1431*, 1–13.

Jackson, G.S., Hosszu, L.L.P., Power, A., Hill, A.F., Kenney, J., Saibil, H., Craven, C.J., Waltho, J.P., Clarke, A.R., and Collinge, J. (1999b). Reversible conversion of monomeric human prion protein between native and fibrilogenic conformations. Science *283*, 1935–1937.

Ji, Z.S., Mullendorff, K., Cheng, I.H., Miranda, R.D., Huang, Y.D., and Mahley, R.W. (2006). Reactivity of apolipoprotein E4 and A-beta peptide: lysosomal stability and neurodegeneration. J. Biol. Chem. *281*, 2683–2692.

Kang, S.C., Brown, D.R., Whiteman, M., Li, R., Pan, T., Perry, G., Wisniewski, T., Sy, M.S., and Wong, B.S. (2004). Prion protein is ubiquitinated after developing protease resistance in the brains of scrapie-infected mice. J. Pathol. *203*, 603–608.

Kayed, R., Head, E., Thompson, J.L., McIntire, T.M., Milton, S.C., Cotman, C.W., and Glabe, C.G. (2003). Common structure of soluble amyloid oligomers implies common mechanism of pathogenesis. Science *300*, 486–489.

Kisselev, A.F., and Goldberg, A.L. (2005). Monitoring activity and inhibition of 26S proteasomes with fluorogenic peptide substrates. Methods Enzymol. *398*, 364–378.

Kisselev, A.F., Kaganovich, D., and Goldberg, A.L. (2002). Binding of hydrophobic peptides to several non-catalytic sites promotes peptide hydrolysis by all active sites of 20S proteasomes. J. Biol. Chem. *277*, 22260–22270.

Kisselev, A.F., Callard, A., and Goldberg, A.L. (2006). Importance of the proteasome's different proteolytic sites and the efficacy of inhibitors varies with the protein substrate. J. Biol. Chem. *281*, 8582–8590.

Klohn, P.C., Stoltze, L., Flechsig, E., Enari, M., and Weissmann, C. (2003). A quantitative, highly sensitive cell-based infectivity assay for mouse scrapie prions. Proc. Natl. Acad. Sci. USA *100*, 11666–11671.

Kovacs, G.G., Preusser, M., Strohschneider, M., and Budka, H. (2005). Subcellular localization of disease-associated prion protein in the human brain. Am. J. Pathol. *166*, 287–294.

Kristiansen, M., Messenger, M.J., Klohn, P.C., Brandner, S., Wadsworth, J.D., Collinge, J., and Tabrizi, S.J. (2005). Disease-related prion protein forms aggresomes in neuronal cells leading to caspase-activation and apoptosis. J. Biol. Chem. *280*, 38851–38861.

Kuwajima, K. (1996). The molten globule state of α-lactalbumin. FASEB J. *10*, 102–109.

Lee, C.K., Weindruch, R., and Prolla, T.A. (2000). Gene-expression profile of the ageing brain in mice. Nat. Genet. *25*, 294–297.

Lindsten, K., Menendez-Benito, V., Masucci, M.G., and Dantuma, N.P. (2003). A transgenic mouse model of the UPS. Nat. Biotechnol. *21*, 897–902.

Lowe, J., Fergusson, J., Kenward, N., Laszlo, L., Landon, M., Farquhar, C., Brown, J., Hope, J., and Mayer, R.J. (1992). Immunoreactivity to ubiquitin-protein conjugates is present early in the disease process in the brains of scrapie-infected mice. J. Pathol. *168*, 169–177.

Ma, J.Y., and Lindquist, S. (2001). Wild-type PrP and a mutant associated with prion disease are subject to retrograde transport and proteasome degradation. Proc. Natl. Acad. Sci. USA *98*, 14955–14960.

Ma, J., and Lindquist, S. (2002). Conversion of PrP to a self-perpetuating PrP^{Sc}-like conformation in the cytosol. Science *298*, 1785–1788.

Mallucci, G.R., Ratté, S., Asante, E.A., Linehan, J., Gowland, I., Jefferys, J.G.R., and Collinge, J. (2002). Post-natal knockout of prion protein alters hippocampal CA1 properties, but does not result in neurodegeneration. EMBO J. *21*, 202–210.

Mallucci, G., Dickinson, A., Linehan, J., Klohn, P.C., Brandner, S., and Collinge, J. (2003). Depleting neuronal PrP in prion infection prevents disease and reverses spongiosis. Science *302*, 871–874.

Pickart, C.M., and Cohen, R.E. (2004). Proteasomes and their kin: proteases in the machine age. Nat. Rev. Mol. Cell Biol. *5*, 177–187.

Prusiner, S.B. (1982). Novel proteinaceous infectious particles cause scrapie. Science *216*, 136–144.

Rubinsztein, D.C. (2006). The roles of intracellular protein-degradation pathways in neurodegeneration. Nature *443*, 780–786.

Sandvig, K., and van Deurs, B. (2002). Membrane traffic exploited by protein toxins. Annu. Rev. Cell Dev. Biol. *18*, 1–24.

Schatzl, H.M., Laszlo, L., Holtzman, D.M., Tatzelt, J., DeArmond, S.J., Weiner, R.I., Mobley, W.C., and Prusiner, S.B. (1997). A hypothalamic neuronal cell line persistently infected with scrapie prions exhibits apoptosis. J. Virol. *71*, 8821–8831.

Sherman, M.Y., and Goldberg, A.L. (2001). Cellular defenses against unfolded proteins. Neuron *29*, 15–32.

Silveira, J.R., Raymond, G.J., Hughson, A.G., Race, R.E., Sim, V.L., Hayes, S.F., and Caughey, B. (2005). The most infectious prion protein particles. Nature *437*, 257–261.

Solforosi, L., Criado, J.R., McGavern, D.B., Wirz, S., Sanchez-Alavez, M., Sugama, S., DeGiorgio, L.A., Volpe, B.T., Wiseman, E., Abalos, G., et al. (2004). Cross-linking cellular prion protein triggers neuronal apoptosis in vivo. Science *303*, 1514–1516.

Verhoef, L.G., Lindsten, K., Masucci, M.G., and Dantuma, N.P. (2002). Aggregate formation inhibits proteasomal degradation of polyglutamine proteins. Hum. Mol. Genet. *11*, 2689–2700.

Voges, D., Zwickl, P., and Baumeister, W. (1999). The 26S proteasome. Annu. Rev. Biochem. *68*, 1015–1068.

Weissmann, C. (2004). The state of the prion. Nat. Rev. Microbiol. *2*, 861–871.

Whitby, F.G., Masters, E.I., Kramer, L., Knowlton, J.R., Yao, Y., Wang, C.C., and Hill, C.P. (2000). Structural basis for the activation of 20S proteasomes by 11S regulators. Nature *408*, 115–120.

Yedidia, Y., Horonchik, L., Tzaban, S., Yanai, A., and Taraboulos, A. (2001). Proteasomes and ubiquitin are involved in the turnover of the wild-type prion protein. EMBO J. *20*, 5383–5391.